# An early secretory pathway mediated by GNOM-LIKE 1 and GNOM is essential for basal polarity establishment in *Arabidopsis thaliana*

Siamsa M. Doyle[a], Ash Haeger[a], Thomas Vain[a], Adeline Rigal[a], Corrado Viotti[b,1], Małgorzata Łangowska[a], Qian Ma[a], Jiří Friml[c,d], Natasha V. Raikhel[e,2], Glenn R. Hicks[e], and Stéphanie Robert[a,2]

[a]Umeå Plant Science Centre, Department of Forest Genetics and Plant Physiology, Swedish University of Agricultural Sciences, 90183 Umeå, Sweden; [b]Umeå Plant Science Centre, Department of Plant Physiology, Umeå University, 90187 Umeå, Sweden; [c]Department of Plant Systems Biology, Vlaams Instituut voor Biotechnologie and Department of Plant Biotechnology and Bioinformatics, Ghent University, 9052 Ghent, Belgium; [d]Institute of Science and Technology Austria, 3400 Klosterneuburg, Austria; and [e]Center for Plant Cell Biology and Department of Botany and Plant Sciences, University of California, Riverside, CA 92521

Spatial regulation of the plant hormone indole-3-acetic acid (IAA, or auxin) is essential for plant development. Auxin gradient establishment is mediated by polarly localized auxin transporters, including PIN-FORMED (PIN) proteins. Their localization and abundance at the plasma membrane are tightly regulated by endomembrane machinery, especially the endocytic and recycling pathways mediated by the ADP ribosylation factor guanine nucleotide exchange factor (ARF-GEF) GNOM. We assessed the role of the early secretory pathway in establishing PIN1 polarity in *Arabidopsis thaliana* by pharmacological and genetic approaches. We identified the compound endosidin 8 (ES8), which selectively interferes with PIN1 basal polarity without altering the polarity of apical proteins. ES8 alters the auxin distribution pattern in the root and induces a strong developmental phenotype, including reduced root length. The ARF-GEF–defective mutants *gnom-like 1* (*gnl1-1*) and *gnom* (*van7*) are significantly resistant to ES8. The compound does not affect recycling or vacuolar trafficking of PIN1 but leads to its intracellular accumulation, resulting in loss of PIN1 basal polarity at the plasma membrane. Our data confirm a role for GNOM in endoplasmic reticulum (ER)–Golgi trafficking and reveal that a GNL1/GNOM-mediated early secretory pathway selectively regulates PIN1 basal polarity establishment in a manner essential for normal plant development.

chemical genomics | endomembrane trafficking | PIN auxin transporters | plasma membrane protein polarity

**D**ue to their sessile lifestyle, the development of plants is characterized by continuous growth, generating the capacity to adapt to environmental conditions. Such flexibility has been made possible by a set of morphological adjustments that are accomplished through altered growth regulation of different plant organs, such as leaves or roots. Most aspects of plant development are regulated by the differential distribution of the plant hormone indole-3-acetic acid (IAA, or auxin) between cells or tissues (reviewed by ref. 1). The formation of auxin maxima is generated concomitantly by local auxin biosynthesis, metabolism, and directional transport (2–8).

Polar auxin transport occurs in a cell-to-cell manner and is dependent on plasma membrane-localized auxin influx and efflux carriers (reviewed by ref. 9). Among them, the PIN-FORMED (PIN) auxin efflux carriers are essential for plant development, and single or multiple *pin* mutants display phenotypes typical for auxin transport defects, such as tropism, embryo development, organogenesis, and root meristem patterning defects (6, 7, 10–14). A polar subcellular localization has been shown for most of the plasma membrane-localized auxin transporters, in particular for the PIN proteins (PIN1-4 and PIN7) and, to some extent, also for the ATP-BINDING CASSETTE SUBFAMILY B proteins (ABCBs) and AUXIN RESISTANT 1 (AUX1) (11–13, 15–20).

The PIN proteins are known to be essential for targeting and redirecting auxin flux, which modulates the spatial pattern of expression of auxin response markers (21). PINs can be targeted toward the apical (shootward), basal (rootward), or lateral plasma membrane depending upon the PIN protein identity, the cell type, and the developmental context (reviewed by ref. 22). In the root, PIN1 is localized basally toward the root tip in stele provascular cells (12). PIN2 is also localized basally in young cortex cells close to the root meristem but is localized apically in mature cortex cells, epidermal cells, and the lateral root cap (16, 22, 23).

Until now, it has been unclear whether newly synthesized PIN proteins are initially secreted to the plasma membrane in a polar or apolar manner. In *Arabidopsis thaliana*, the current model for PIN polar localization establishment and maintenance at the plasma membrane is based on endocytosis, polar recycling, and restriction of lateral diffusion (reviewed by ref. 24). PIN proteins are internalized via clathrin-mediated endocytosis (25, 26) and can cycle back to plasma membrane domains via distinct trafficking routes. Recycling and endocytosis of PIN1 depend on the endosome-localized fraction of the ADP ribosylation factor guanine nucleotide exchange factor (ARF-GEF) GNOM (27,

## Significance

Within plants, controlled gradients of the hormone auxin are essential for development. These gradients are achieved through intracellular polar positioning of auxin transporter proteins, such as PIN-FORMED proteins (PINs), at the plasma membrane, thus guiding the direction of auxin transport. The establishment and maintenance of PIN polarity is controlled within each cell by complicated trafficking pathways of the endomembrane system. In the model plant *Arabidopsis*, it has long been known that endocytosis and recycling trafficking routes play roles in PIN polarity. In this study, we reveal the role of a secretory route in this process. Our evidence shows that this secretory trafficking route selectively controls basal (rootward) but not apical (shootward) PIN polarity.

28), which is sensitive to the fungal toxin brefeldin A (BFA) (29). ARF-GEFs are essential regulators of vesicle formation and, among the eight ARF-GEFs in *Arabidopsis*, GNOM is the only one reported as being essential specifically for basal PIN recycling, whereas apical PIN and AUX1 localization and dynamics are not affected in *gnom* mutants (30, 31). Additionally, although apical targeting of AUX1 is resistant to BFA, subcellular AUX1 trafficking is BFA-sensitive, suggesting that trafficking of apical proteins may require both BFA-sensitive and -insensitive, GNOM-independent, ARF-GEF–mediated pathways (30, 32).

In addition to GNOM, other *Arabidopsis* ARF-GEFs have been characterized, including GNOM-LIKE 1 (GNL1), which localizes to Golgi stacks and is BFA-resistant (33, 34). GNL1 acts in the early secretory pathway where it regulates COPI-mediated recycling of endoplasmic reticulum (ER)–resident proteins from the Golgi back to the ER (33, 34). Moreover, GNOM has recently been shown to predominantly localize to Golgi stacks (35) where it plays a minor but redundant function to GNL1 in ER-Golgi trafficking (33). The other *Arabidopsis* ARF-GEFs include GNL2, which is expressed specifically in pollen (36), and the five BIG ARF-GEFs, BIG1 to -5. BIG5, which is BFA-sensitive, has been described under the name BFA-VISUALIZED ENDOCYTIC TRAFFICKING DEFECTIVE 1 (BEN1) as mediating early endosomal trafficking (37). BIG1 to -4, of which BIG3 is BFA-resistant whereas BIG1, -2, and -4 are BFA-sensitive, have recently been described as acting redundantly in the late secretory pathway from the trans Golgi network (TGN) to the plasma membrane, as well as in late vacuolar trafficking (38).

Endosomal PIN homeostasis is tightly controlled by the retromer complex through the regulation of PIN protein trafficking to the vacuole, thus controlling polar PIN abundance within the cell (39–43). Additionally, a large amount of data has demonstrated that not only trafficking routes per se are essential to determine the polar localization of PIN proteins but also internal protein signals such as posttranslational phosphorylation via the protein kinase PINOID (PID) and the protein phosphatase 2A (PP2A) (44–46). Despite recent progress, our understanding of the mechanisms establishing basal polarity remains limited. In the present work, we aimed to unravel the details of PIN basal polarity establishment by identifying selective inhibitors of this process.

A number of genetic screens have been successfully used to discover new components of the endomembrane system (for examples, see refs. 34, 37, and 47–51). However, most of the molecular actors regulating endomembrane trafficking are either essential to plant survival or belong to large protein families, leading to lethality of knock-out mutants or lack of a phenotype due to redundancy. The use of fast-acting molecules suitable for the highly dynamic nature of the endomembrane system circumvents these problems and has deepened our understanding of interconnected networks of trafficking routes (52–58). While BFA has expanded our knowledge of the GNOM-dependent recycling pathway (27), other small compounds can be used to dissect different trafficking routes. In recent studies, automated screening of small molecules based on inhibition of tobacco pollen tube growth led to the isolation of a set of compounds interfering with the endomembrane system (52). Through the screening of 46,418 diverse molecules, 360 were identified as inhibitors of pollen germination (53). To dissect the trafficking routes of plasma membrane proteins specifically, a secondary screen was established based on confocal laser-scanning microscopy, leading to the identification of 123 compounds named plasma membrane recycling compound A (PMRA), which induce mislocalization of plasma membrane markers in the *Arabidopsis* root meristem (53).

In the present study, we reasoned that using the PMRA endomembrane trafficking modulators in combination with BFA could unravel trafficking routes regulating basal plasma membrane targeting. We designed a chemical screen to identify PMRA molecules that modulated the accumulation of PIN1 in BFA-induced agglomerations. We subsequently identified the endosidin 8 (ES8) compounds, including the original compound ES8.0 and its more potent analog ES8.1, which selectively modify PIN1 basal plasma membrane targeting in *Arabidopsis* with minimal effects on apical plasma membrane proteins. Using this pharmacological approach, we herein confirm that GNOM plays a role in ER-Golgi trafficking independently of its role in recycling and reveal that a GNL1/GNOM-dependent early secretory pathway is essential for targeting PIN1 toward the basal plasma membrane. Furthermore, we demonstrate that this pathway is specific for basal polarity establishment, revealing an essential and previously unknown regulatory mechanism for establishing cell polarity and regulating auxin transport and plant development.

## Results

### Identification of Endosidin 8, a Compound Affecting PIN1 Trafficking.
We reasoned that screening for chemical activity affecting trafficking of basally localized plasma membrane proteins would allow us to elucidate mechanisms regulating basal polarity establishment. We therefore designed a chemical screen to identify compounds causing a decrease in accumulation of endogenous basal PIN1 in BFA bodies (BFA-induced agglomerations) (59) in the *Arabidopsis* root. We screened the PMRA collection, a set of compounds already identified as affecting plasma membrane protein trafficking (53) and isolated the compound ES8.0 (ES8 version 0) (Fig. 1*A*). In comparison with mock treatment and in a dose-dependent manner, 6 and 10 µM ES8.0 vastly reduced the number of PIN1-labeled BFA bodies in provascular cells by 20% and 60%, respectively (Fig. 1 *B* and *C*), suggesting interference of the compound with PIN1 trafficking routes. We then demonstrated that this interference with trafficking was not related to visible defects in the morphologies of endomembrane compartments, such as ER, Golgi apparatus, TGN, or multivesicular bodies (prevacuolar compartments) (Fig. S1 *A–C*). We furthermore showed that ES8.0 had no effect on BFA-induced agglomerations per se, as shown by the uptake of the styryl dye FM4-64 into BFA bodies (Fig. S1*D*), and that the effect of ES8.0 on PIN1 trafficking was not related to detectable cytoskeleton modifications (Fig. S1 *E* and *F*).

We conducted a structure-activity relationship study to better understand the essential structural determinants of ES8.0 bioactivity on PIN1 trafficking. Six close structural analogs of the molecule hereby named ES8.1 to ES8.6 (Fig. S2*A*) were tested for their effects on BFA sensitivity of PIN1 at 10 µM (Fig. S2 *B* and *C*). Two of the analogs, ES8.2 and ES8.3, showed an effect that was not significantly different to that of ES8.0. The analogs ES8.4, ES8.5, and ES8.6 showed a weaker effect than ES8.0. These analogs mainly differed structurally from ES8.0 with respect to the presence and positions of halogens on the phenolic rings. Additionally, ES8.4 contained a thiophene ring in place of a phenolic ring found in ES8.0. The analog ES8.1 (Fig. 1*A*) showed a more potent effect than ES8.0, reducing PIN1-labeled BFA body number by 70% compared with the control. This higher potency was also confirmed at the lower concentration of 6 µM (Fig. 1 *B* and *C*). Importantly, like ES8.0, ES8.1 did not visibly affect the morphology of the Golgi apparatus, the TGN, or multivesicular bodies in provascular cells (Fig. S2*D*), nor did ES8.1 have any effect on BFA-induced agglomerations per se (Fig. S2*E*). These results indicate that the positions of the halogens are critical for the potency of ES8 activity. The phenolic ring containing a carboxyl group is also particularly important for activity. Overall, we have isolated ES8.0 and its stronger analog ES8.1 as compounds interfering with the accumulation of PIN1 in BFA bodies without visibly affecting the morphology of the endomembrane trafficking network.
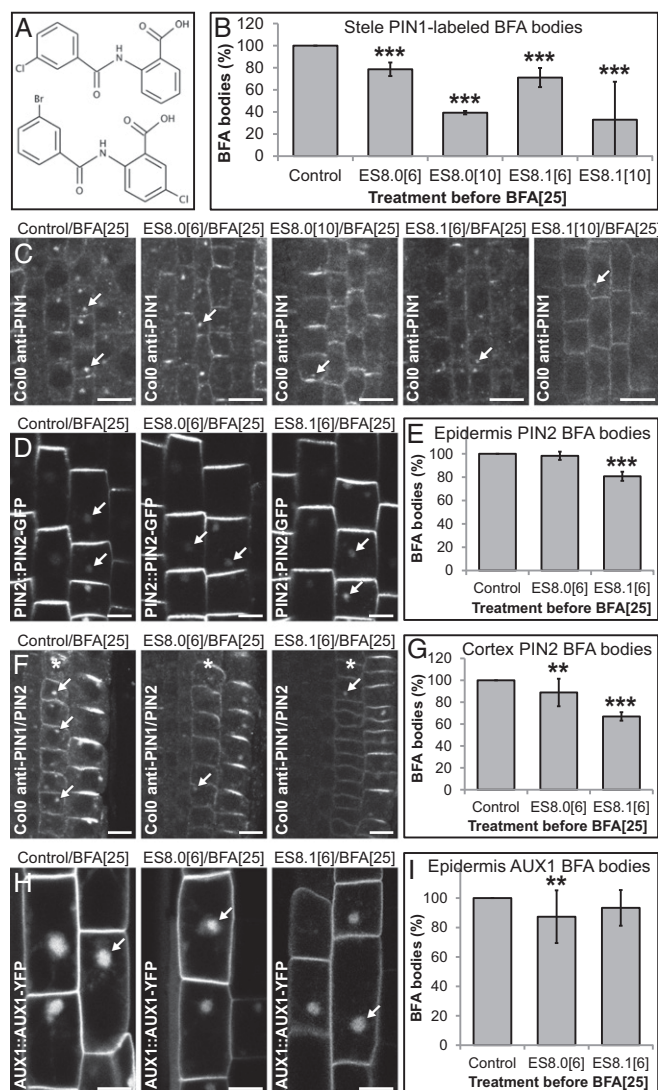
**Fig. 1.** ES8 preferentially interferes with trafficking of basal plasma membrane proteins. (A) Chemical structures of ES8.0 (*Top*) and ES8.1 (*Bottom*). (B and C) PIN1-labeled BFA bodies in stele cells of anti-PIN1 immunolocalized Col0 roots. (D and E) PIN2-GFP–labeled BFA bodies in epidermis cells of PIN2::PIN2-GFP roots. (F and G) PIN2-labeled BFA bodies in cortex cells of anti-PIN2 immunolocalized Col0 roots. (H and I) AUX1-YFP–labeled BFA bodies in epidermis cells of AUX1::AUX1-YFP roots. Representative images are shown. (Scale bars: 10 μm.) Arrows mark BFA bodies. Asterisks mark cortex cell files. Values in square brackets indicate treatment concentrations in μM. Quantification is calculated as the number of bodies per cell cross-section and expressed as a percentage of the control mock treatment in each replicate with $n > 600$ (B and G) or 300 (E and I) cells. Indicated treatments were significantly different to the control with $P < 0.01$ (**) or $P < 0.0001$ (***), as calculated using the Wilcoxon rank sum (Mann–Whitney U) test. Error bars represent SD.

**Establishment of PIN1 Basal Polarity Requires a Distinct Trafficking Pathway.** To investigate whether the ES8 compounds preferentially interfere with trafficking of basal proteins, their effects on BFA-induced agglomeration of apical and basal PIN2, apolar AUX1, and apical PIN1 were examined. Interestingly, apical PIN2-GFP in the epidermis was completely resistant to ES8.0 whereas the analog ES8.1 reduced the accumulation of this protein in BFA bodies (Fig. 1 D and E). In contrast, BFA-induced agglomeration of basal endogenous PIN2 in the cortex was sensitive to both ES8.0 and ES8.1 (Fig. 1 F and G). We then tested the effects of the compounds on another auxin transporter, AUX1,

which localizes mainly apolarly in epidermal cells, with some higher accumulations at both the basal and apical plasma membranes (30). ES8.0 modestly reduced the number of AUX1-YFP–labeled BFA bodies in the epidermis (Fig. 1 H and I). The effects of the compounds on apolar AUX1-YFP were intermediate between those on apical and basal proteins, as confirmed by comparison of AUX1-YFP and PIN2-GFP BFA body size after treatment (Fig. S3 A and B), leading us to presume that only the basally localized pool of AUX1-YFP is ES8-sensitive. We then investigated the effects of the ES8 compounds in the protein kinase PINOID-overexpressing line 35S::PID21 in which PIN1 is apically localized in root provascular cells (44). Although the BFA sensitivity of PIN1 in this line is already substantially reduced in comparison with the WT (46), BFA did induce some PIN1-labeled agglomerations in our conditions, quantification of which revealed that apical PIN1 BFA sensitivity was totally unaffected by ES8.1 (Fig. S3 C–E). Collectively, these results demonstrate that the ES8 compounds preferentially interfere with basal trafficking of plasma membrane proteins.

We further tested the direct effects of the ES8 compounds on the polarity of PIN1 and PIN2. Quantitative analysis of endogenous PIN1 basal-to-lateral plasma membrane signal ratio in the stele revealed that ES8.1 severely compromised PIN1 basal polar localization (Fig. 2 A and B). In contrast, neither of the ES8 compounds reduced PIN2 apical polar localization in the epidermis (Fig. 2 C and D). ES8.0 slightly increased apical polarity of epidermal PIN2, which we presume reflects a reduction in PIN2 abundance at the basal ends of the lateral plasma membranes. We also observed some intracellular accumulation of PIN1 signal after treatment with the compounds, especially ES8.1 (Fig. 2A). These results demonstrate that the ES8 compounds selectively disrupt trafficking mechanisms involved in basal polarity establishment, confirming the existence of distinct trafficking routes determining apical and basal polarity.

**A Trafficking Route Regulated by GNL1 and GNOM Is Involved in the PIN1 Basal Polarity Establishment Required for Plant Development.** We observed that the physiological effects of the ES8 compounds on seedling growth, including reduced root length and root
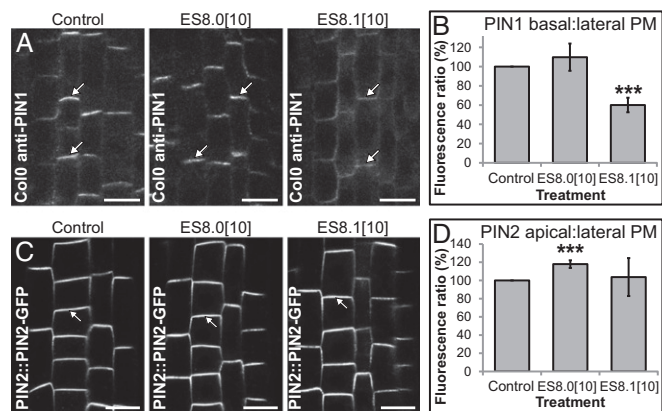


**Fig. 2.** ES8 selectively interferes with basal polarity establishment. (A and B) PIN1 basal polarity in stele cells of anti-PIN immunolocalized Col0 roots. (C and D) PIN2-GFP apical polarity in epidermis cells of PIN2::PIN2-GFP roots. Representative images are shown. (Scale bars: A, 10 μm; C, 20 μm.) Arrows mark basal (A) or apical (C) plasma membrane (PM). Values in square brackets indicate treatment concentrations in μM. Quantification is calculated as the ratio of basal/apical to lateral PM fluorescence per cell and expressed as a percentage of the control mock treatment in each replicate with $n > 300$ (B) or 150 (D) cells. Indicated treatments were significantly different to the control with $P < 0.0001$ (***), as calculated using the Wilcoxon rank sum (Mann–Whitney U) test. Error bars represent SD.

agravitropism, were reminiscent of mutants defective in auxin-mediated mechanisms. Germination and growth of seedlings on plates supplemented with ES8.0 led to uniform inhibition of shoot and root growth compared with growth on mock-treated plates (Fig. 3 *A* and *B*). These effects were remarkably stronger in the absence of sucrose in the medium (Fig. S4 *A* and *B*), an observation that has been noted before for several trafficking-defective mutants (37, 42, 60, 61). The effect of ES8.1 on seedling growth was stronger and differential, resulting in a range of defective root growth and gravitropism phenotypes, including occasional total absence of root development (Fig. 3 *A* and *B*).

The short root phenotype, together with reduced PIN1 polarity in the stele, suggests that ES8 induces defects in auxin distribution in the root. To test this possibility, we studied the effects of the ES8 compounds on distribution of the auxin-responsive promoter *DR5* in roots of DR5rev::GFP seedlings (11). Observations of *DR5* expression patterns in full roots of seedlings germinated and grown directly on ES8-supplemented medium revealed clearly decreased signals in the steles compared with control seedlings (Fig. S4 *C–E*). Detailed observations of the root tips revealed ES8-induced accumulations of *DR5* signals, extended into cell file initials surrounding the quiescent center, which were not labeled in control conditions (Fig. S4 *F–H*). These results suggest that ES8-induced PIN1 localization and polarity defects in the stele lead to altered auxin distribution and auxin accumulation in the root tip, which in turn lead to inhibited root growth.

To gain further insights into the ES8-targeted trafficking mechanisms involved in regulating basal polarity, we screened available trafficking mutants for altered ES8 sensitivity. We found that the ARF-GEF mutants *gnl1-1* and *vascular network 7* (*van7*, a partial loss-of-function allele of *GNOM*) were significantly resistant to the effects of ES8.0 on root length compared with the WT (Fig. 3 *C–E*). These mutants did not seem to be resistant to ES8.1; however, it may be that the highly differential effect of ES8.1 on root length may have hindered detection of mutant resistance to this compound. Other trafficking mutants, including *ben1-1*, *sorting nexin 1–1* (*snx1-1*), *vacuolar protein sorting 29–3* (*vps29-3*), and *osmotic stress-sensitive mutant 1* (*osm1*), did not show any altered sensitivity to either of the ES8 compounds (Fig. S5*A*). The reduced sensitivities of *gnl1-1* and *van7* mutants to the ES8 compounds imply that the trafficking pathways that are defective in these mutants might be targeted by the compounds. These results therefore suggest that the ES8 compounds might selectively target trafficking pathways regulated by GNL1 and/or GNOM.

It has previously been shown that, in *gnl1-2* mutants, PIN1 is less sensitive to BFA than in the WT (34), an effect that we seem to have mimicked in the WT by ES8 treatment. In line with this finding, we found that *gnl1-1* also produced less BFA-induced PIN1 agglomerations than the WT (Fig. 3 *G* and *H*). These results tend to agree with our suggestion that the ES8 compounds target a GNL1-regulated pathway, thereby also reducing PIN1-labeled BFA body formation. We next investigated the altered ES8 sensitivity of *gnl1-1* at the cellular level, revealing resistance of the mutant to the inhibitory effects of the ES8 compounds on PIN1 accumulation in BFA bodies compared with the WT (Fig. 3 *F–H*). The mutant *van7* could not be investigated in this way because BFA is not effective in inducing agglomerations when GNOM function is compromised, as previously demonstrated in the mutant *gnom*$^{R5}$, another partial loss-of-function allele of *GNOM* (62). We found that, although PIN1-labeled agglomerations were induced in the root tips of the *van7* WT background, almost no agglomerations were induced in *van7* (Fig. S5 *B* and *C*).

The ES8 compounds induce PIN1 polarity defects (Fig. 2 *A* and *B*). Similarly, *gnom* mutants have been shown to have severe PIN1 polarity defects (29) due to the importance of GNOM for PIN1 recycling (27) and endocytosis (28) at the plasma membrane. We next investigated endogenous PIN1 polarity in the *gnl1-1* mutant. Analysis of PIN1 basal-to-lateral plasma membrane signal ratio revealed a subtle yet highly significant reduction in PIN1 polar localization compared with the WT (Fig. 3I), suggesting that GNL1 plays a role in PIN1 basal polarity. The fact that this polarity defect is slight and weaker than that induced in the WT by ES8.1 suggests redundancy between GNL1 and GNOM in the trafficking pathway targeted by the ES8 compounds. Together, these data reveal that a specific trafficking pathway involving GNL1 and GNOM is involved in basal plasma membrane targeting of PIN1.

**An Early Secretory Trafficking Pathway Toward the Plasma Membrane Is Essential for PIN1 Basal Polarity Establishment.** Because GNOM-regulated trafficking between endosomes and the
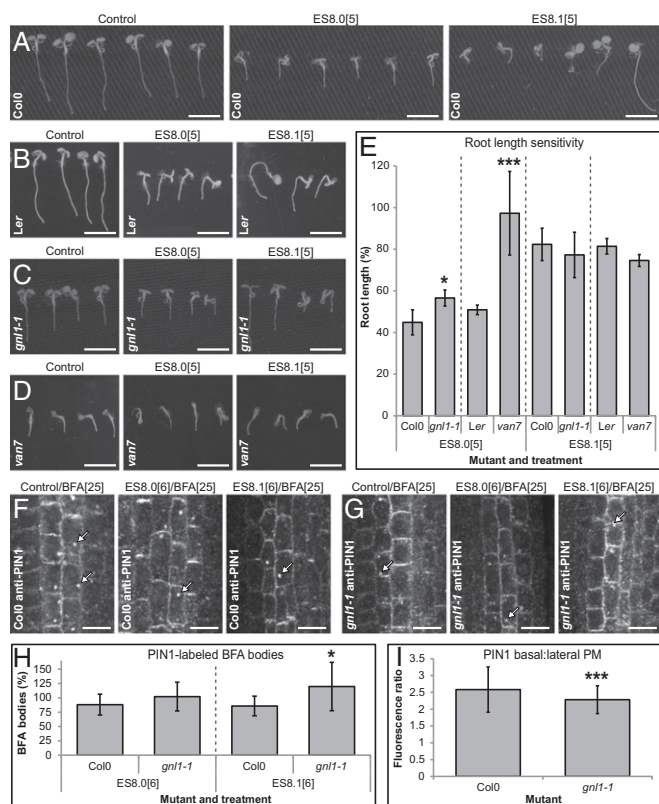


**Fig. 3.** A GNL1/GNOM-mediated trafficking pathway is involved in establishing PIN1 basal polarity. (*A–E*) Root-length sensitivity of Col0 (*A*), Ler (*B*), *gnl1-1* (*C*), and weak *gnom* mutant *van7* (*D*) to the ES8 compounds. Seedlings were germinated and grown for 5 d on treatment-supplemented growth medium. Due to heterozygosity of *van7*, seedlings lacking a fused cotyledon phenotype were cropped out of these images (*D*) and excluded from root-length measurements (*E*). Quantification is expressed as a percentage of the control mock treatment per mutant in each replicate with *n* > 90 seedlings. (*F–H*) PIN1-labeled BFA bodies in stele cells of anti-PIN1 immunolocalized Col0 (*F*) and *gnl1-1* (*G*) roots. Quantification is calculated as the number of bodies per cell cross-section and expressed as a percentage of the control mock treatment per mutant in each replicate with *n* > 600 cells. (*I*) PIN1 basal polarity in stele cells of anti-PIN1 immunolocalized Col0 and *gnl1-1* roots, calculated as the ratio of basal to lateral plasma membrane (PM) fluorescence per cell and expressed as a percentage of the WT in each replicate with *n* > 300 cells. Representative images are shown. (Scale bars: *A–D*, 5 mm; *F* and *G*, 10 μm.) Arrows mark BFA bodies. Values in square brackets indicate treatment concentrations in μM. Indicated treatments were significantly different to the WT with $P < 0.05$ (*) or $P < 0.0001$ (***), as calculated using the Student's *t* test (*E* and *H*) or Wilcoxon rank sum (Mann–Whitney *U*) test (*I*). Error bars represent SD.

plasma membrane has been shown to be a crucial process influencing establishment and maintenance of PIN basal polar localization at the plasma membrane (27, 29, 63), we investigated the effects of the ES8 compounds on endocytosis and exocytosis. We first investigated the general endocytosis pathway by analyzing the intracellular accumulation of the endocytic tracer FM4-64 (64). Neither ES8.0 nor ES8.1 treatment altered internalization of FM4-64 compared with the mock treatment (Fig. 4 *A* and *B*). Previous work has shown that PIN proteins are cargos of the clathrin-mediated endocytosis pathway (25). We thus tested the activities of the ES8 compounds on CLATHRIN LIGHT CHAIN 2 (CLC2) localization. CLC2-GFP labeled the plasma membrane and was associated with intracellular compartments (most likely TGN) (65) both in the absence and presence of each of the ES8 compounds (Fig. 4 *C* and *D*). We then investigated exocytosis of endogenous PIN1 by performing BFA washouts in the presence of the ES8 compounds. Washing

after BFA treatment removes the compound's inhibitory effect on exocytosis, causing BFA bodies to dissipate (59). Compared with BFA treatment before washing, washouts with either ES8.0 or ES8.1 reduced BFA body number and size similar to control washout (Fig. 4 *E* and *F*). To further analyze the effects of the compounds on the endocytic and recycling machinery, we investigated whether they modify early endosome identity by testing the degree of colocalization of TGN markers in the absence and presence of the compounds. Colocalization of Syntaxin of Plants 61 (SYP61) with either Rab-GTPase A2a (RABA2a) or Vacuolar H$^+$-ATPase subunit a1 (VHA-a1) was not modified by the ES8 compounds (Fig. S6). Together, these data demonstrate that the ES8 compounds modify basal PIN1 trafficking without affecting the endocytic or exocytic machinery.

It has been shown that targeting of PINs to the vacuole for degradation is also involved in regulating the abundance and localization of these proteins (22). We therefore investigated
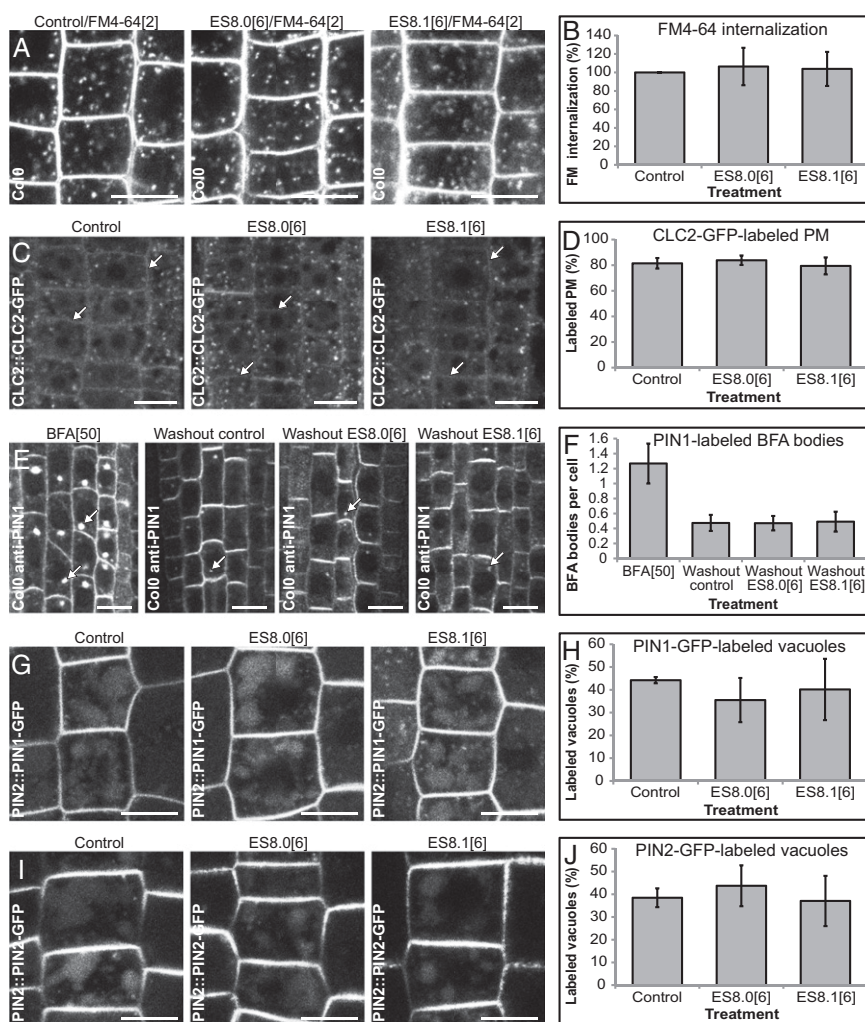


**Fig. 4.** ES8 does not affect clathrin-mediated endocytosis, exocytosis, or vacuolar trafficking. (*A* and *B*) Endocytic FM4-64 internalization 5 min after labeling in epidermis cells of Col0 roots. Quantification is calculated as the ratio of plasma membrane (PM) to intracellular epidermal cell FM4-64 fluorescence and expressed as a percentage of the control mock treatment in each replicate with *n* > 180 cells. (*C* and *D*) Clathrin labeling of PM in epidermis cells of CLC2::CLC2-GFP roots. Quantification is expressed as the percentage of epidermal cells per root with CLC2-GFP visible at the PM in each replicate with *n* > 30 roots. (*E* and *F*) PIN1-labeled BFA bodies in stele cells of anti-PIN1 immunolocalized Col0 roots. Quantification is calculated as the number of bodies per cell cross-section with *n* > 600 cells. (*G* and *H*) Accumulation of PIN1-GFP in epidermis cell vacuoles of PIN2::PIN1-GFP roots. Quantification is expressed as the percentage of epidermal cells per root showing GFP visible inside vacuoles with *n* > 30 roots. (*I* and *J*) Accumulation of PIN2-GFP in epidermis cell vacuoles of PIN2::PIN2-GFP roots. Quantification is expressed as the percentage of epidermal cells per root showing GFP visible inside vacuoles with *n* > 30 roots. Representative images are shown. (Scale bars: 10 μm.) Arrows mark PM (*C*) or BFA bodies (*E*). Values in square brackets indicate treatment concentrations in μM. No statistically significant differences were found between treatments. Error bars represent SD.

whether vacuolar trafficking pathways are affected by the ES8 compounds by incubating seedlings of PIN1-GFP and PIN2-GFP lines in darkness to allow visualization of GFP signal in the vacuoles as reported previously (42, 66, 67). PIN1-GFP (Fig. 4 *G* and *H*) and PIN2-GFP (Fig. 4 *I* and *J*) accumulated similarly in the vacuoles of mock-treated, ES8.0-treated, and ES8.1-treated seedlings, indicating that the ES8 compounds do not interfere with vacuolar-targeted trafficking.

GNL1 plays an important role in ER-Golgi trafficking (33, 34), and evidence suggests that GNOM is also involved in the early secretory pathway (33). We therefore addressed whether PIN1 basal polarity establishment involves secretory trafficking of the newly produced protein toward the plasma membrane. We studied the effects of the ES8 compounds on newly synthesized PIN1 in the XVE::PIN1 line in which overexpression of PIN1 is inducible (68). Induction of PIN1 synthesis simultaneously with ES8 treatment revealed a reduction in basal plasma membrane-localized abundance of newly produced endogenous PIN1 by both ES8 compounds (Fig. 5 *A* and *B*). In these experiments the ES8 compounds also reduced lateral membrane-localized PIN1 abundance (Fig. S7*A*) and, consistent with our previous results, reduced PIN1 basal polarity (Fig. S7*B*). These data strongly suggest that ES8.0 and ES8.1 specifically target a secretory pathway that delivers newly produced PIN1 toward the basal plasma membrane and that this route is essential for basal polarity establishment.

The strong reduction in PIN1 accumulation both in BFA bodies and at the plasma membrane by ES8 treatment led us to investigate whether de novo production of PIN1 is defective in ES8-treated roots. We therefore performed whole-cell photobleaching in the stele of PIN1-GFP root tips to analyze newly synthesized PIN1-GFP secretory trafficking through the cell to the plasma membrane without contribution from the recycling pathway. We then quantified whole-cell (including both intracellular and plasma membrane), as well as separate intracellular and plasma membrane, fluorescence recovery after photobleaching (FRAP). Remarkably, PIN1-GFP whole-cell fluorescence recovered significantly faster in ES8-treated than mock-treated conditions (Fig. 5*C*) whereas PIN2-GFP whole-cell fluorescence recovered similarly in all conditions (Fig. S7*C*). These results lead us to conclude that, whereas the ES8 compounds do not affect PIN2 trafficking, they modify PIN1 trafficking without suppressing its de novo synthesis. In agreement with this conclusion, the compounds did not modify the transcription of *PIN1*, *PIN2*, or *AUX1* compared with mock treatment (Fig. 5*D*). Furthermore, although intracellular and plasma membrane recovery of PIN1-GFP fluorescence after photobleaching was not significantly different in mock-treated conditions (Fig. S7*D*), intracellular recovery was significantly faster than plasma membrane recovery in ES8-treated conditions (Fig. S7 *E* and *F*).

Our results show that, whereas the ES8 compounds decrease newly synthesized PIN1 localization at the plasma membrane, they also increase intracellular but not plasma membrane PIN1 recovery rate after photobleaching. We reasoned that the ES8-induced increased recovery rate of PIN1 must therefore be due to the intracellular accumulation of PIN1, which we had previously observed by immunolocalization (Fig. 2*A*), in line with inhibited trafficking of the protein toward the plasma membrane. Detection of intracellular immunolocalized PIN1 labeling is limited in detail due to the fixation process. We therefore investigated intracellular PIN1 further by examining the effects of the ES8 compounds on PIN1-GFP in the stele of living root tips. Strikingly, the ES8 compounds induced obvious visible accumulation of intracellular PIN1-GFP signal in provascular cells in a pattern resembling the ER network (Fig. 5*E*). Quantitative analysis of PIN1-GFP basal plasma membrane-to-intracellular signal ratio confirmed our observations, revealing significantly more internal compared with basal signal after ES8 treatment in comparison
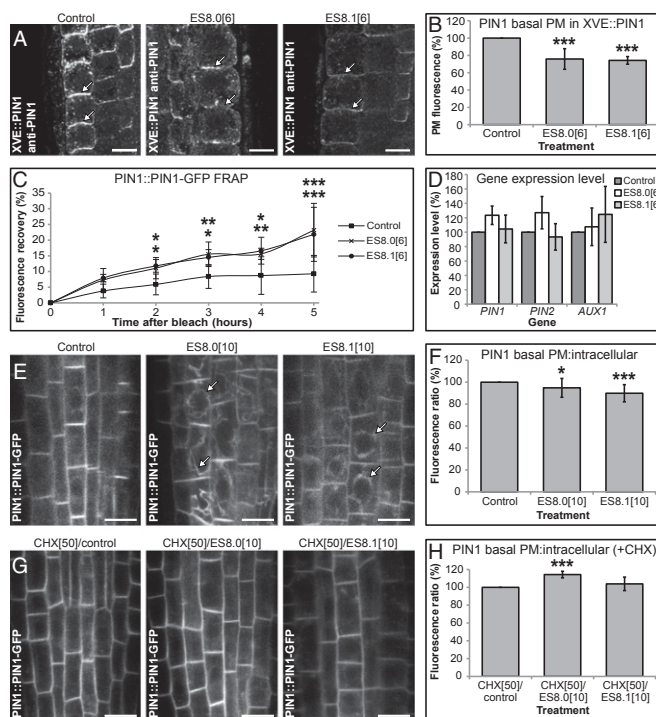


**Fig. 5.** ES8 interferes with a PIN1 secretory pathway toward the basal plasma membrane without affecting its biosynthesis or *PIN1* expression. (*A* and *B*) Basal plasma membrane (PM) fluorescence in epidermis cells of anti-PIN1 immunolocalized XVE::PIN1 roots. Quantification is expressed as a percentage of the control mock treatment in each replicate with n > 150 cells. (*C*) Whole-cell fluorescence recovery after photobleaching (FRAP) in stele cells of PIN1::PIN1-GFP roots with n > 6 roots. (*D*) Expression level of genes *PIN1*, *PIN2*, and *AUX1* in Col0 seedlings. Quantification is expressed as a percentage of the control mock treatment in each replicate. (*E–H*) ES8-induced agglomerations in stele cells of PIN1::PIN1-GFP roots (*E* and *F*) and their inhibition by pretreatment with cycloheximide (CHX) (*G* and *H*). Quantification is calculated as the ratio of basal PM to intracellular fluorescence per cell and expressed as a percentage of the control mock treatment in each replicate with n > 150 cells. Representative images are shown. (Scale bars: 10 μm.) Arrows mark basal PM (*A*) or ES8-induced agglomerations (*E*). Values in square brackets indicate treatment concentrations in μM. Indicated treatments were significantly different to the control with $P < 0.05$ (*), $P < 0.01$ (**), or $P < 0.0001$ (***), as calculated using the Wilcoxon rank sum (Mann–Whitney $U$) test (*B*, *F*, and *H*) or the Student's $t$ test (*C*). Upper and lower asterisks correspond to ES8.0 and ES8.1, respectively in *C*. No significant differences were found between treatments in *D*. Error bars represent SD.

with mock treatment (Fig. 5*F*). Furthermore, no intracellular accumulation of PIN1-GFP was observed when the experiment was performed in the presence of cycloheximide (Fig. 5 *G* and *H*) although, interestingly, cotreatment of ES8.0 with cycloheximide affected the PIN1-GFP basal plasma membrane-to-intracellular ratio (Fig. 5*H*). In contrast to PIN1-GFP, we never observed ER-like accumulation of intracellular PIN2-GFP signal in the epidermis after ES8 treatment (Fig. 2*C*).

These results reveal that establishment of PIN1 basal polarity is dependent on secretory trafficking of the protein toward the basal plasma membrane and that the ES8 compounds inhibit this trafficking pathway without affecting gene expression or protein biosynthesis. Collectively the results of this study confirm that GNOM plays a role in early secretion and reveal that the early secretory trafficking pathway regulated by GNL1/GNOM is crucial for establishing basal polarity at the plasma membrane, while not seeming to play a role in apical polarity establishment. Furthermore, the role played by this secretory pathway in PIN1 basal

polarity establishment is essential for normal auxin distribution and plant development, including root growth and gravitropic response.

## Discussion

**Endosidin 8 Is a New Chemical Tool Specifically Targeting Early Secretory Trafficking.** In this study, we have identified and characterized the compounds ES8.0 and its analog ES8.1 as tools holding great potential toward unraveling the endomembrane trafficking pathways operating in plant cells. The dynamic and complex nature of these essential trafficking routes presents some limitations to the use of genetic studies in dissecting them in vivo. Fast-acting small molecules continue to overcome many of these limitations and have greatly enhanced our understanding of endomembrane transport (reviewed by ref. 69). The specificity of the ES8 compounds has enabled us to uncover an unexpected and essential function of the early secretory trafficking pathway mediated by GNL1 and GNOM in the establishment of PIN1 basal polarity.

Our work shows that the ES8 compounds act in a fast and dose-dependent manner and specifically interfere with the early secretory trafficking pathway toward the basal plasma membrane without inducing visible changes in endomembrane compartment morphology or cytoskeletal integrity. Additionally, endocytic, exocytic, and vacuolar trafficking pathways remain unaffected. This selective activity contrasts with that of other known compounds that have already greatly contributed toward our understanding of endomembrane trafficking and cell polarity. Although compounds such as 2,3,5-triiodobenzoic acid (TIBA), 2-(1-pyrenoyl) benzoic acid (PBA), and latrunculins inhibit general endomembrane trafficking via interference with cytoskeletal actin filaments (59, 70), we have shown that no such activity exists for the ES8 compounds. Neither do the ES8 compounds interfere with endocytosis, unlike the compound ES1, which selectively inhibits endocytic pathways (52, 69), and tyrphostin A23, which prevents cargo uptake into clathrin-coated vesicles (25, 71). Perhaps more similar to ES8 is the recently isolated compound LG8, which also interferes with secretion to the plasma membrane, but probably at the level of the TGN. However, unlike ES8, LG8 results in dramatic morphological changes to ER and Golgi (58).

BFA, the most commonly used compound for endomembrane research, specifically targets several ARF-GEFs and, unlike ES8, subsequently interferes with multiple endocytic, exocytic, and secretory trafficking routes (27, 71, 72). In contrast, the ES8 compounds do not interfere with multiple trafficking routes. ES8 does not indiscriminately target the *Arabidopsis* ARF-GEFs, as demonstrated by the different sensitivities of various ARF-GEF mutants to the compounds. Although mutants defective in GNL1 and GNOM are resistant to ES8, those defective in BIG5 display sensitivity similar to the WT. The unaltered sensitivities of the mutants *snx1-1* and *vps29-3*, which are defective in proteins involved in vacuolar trafficking (41, 43), and the mutant *osm1*, which is defective in the syntaxin SYP61 (47), confirm the specificity of ES8 in targeting the early secretory pathway. Our work shows that, uniquely compared with other known compounds, the ES8 compounds preferentially target a basal membrane-specific early secretory trafficking pathway without inducing any observable cellular morphological phenotypes.

**The GNL1/GNOM-Regulated Early Secretory Pathway Establishes Basal PIN1 Polarity.** The ES8 compounds inhibit PIN1 basal trafficking, leading to altered auxin distribution in the root stele, implying reduced PIN1-mediated shoot-to-root auxin transport. The compounds also lead to accumulation of auxin in the root tip, perhaps due to auxin biosynthesis feedback mechanisms or disturbed trafficking of other auxin transporter proteins, in a pattern similar to that induced by the auxin transport inhibitors *N*-1-naphylphthalamic acid (NPA) and 2-(4-[diethylamino]-2-hydroxybenzoyl)

benzoic acid (BUM) (73, 74). These changes in auxin distribution lead to severely reduced root length and root agravitropic defects, which are also the phenotypes resulting from NPA and BUM treatment at similar concentrations to ES8 (74).

Taken together, our work reveals an essential GNL1 and GNOM-regulated mechanism for establishing PIN1 polarity, thereby controlling auxin transport and auxin-mediated plant development, including root growth and gravitropism. Multiple trafficking pathways in *Arabidopsis* are mediated by GNL1 and GNOM, members of the Golgi-specific BFA resistance factor 1 (GBF1) clade of *Arabidopsis* ARF-GEF proteins (reviewed by ref. 75). In mammals and yeast, the GBF1 clade ARF-GEFs perform conserved, ancestral functions in regulating ER-Golgi trafficking (reviewed by refs. 75 and 76); however, in *Arabidopsis*, the BFA-sensitive ARF-GEF GNOM (29) is required for the recycling of PIN1 between endosomes and the plasma membrane (27), a function that seems to have evolved divergently in plants. The closest homolog of GNOM in *Arabidopsis* is GNL1, which is insensitive to BFA and localizes to the Golgi, where it performs the ancestral function of mediating ER-Golgi transport (33, 34). Our study demonstrates that the ES8 compounds interfere with the targeting of PIN proteins to the basal plasma membrane and lead to intracellular agglomeration of PIN1, possibly in the ER network. It is already well-established that apical and basal targeting of cargo proteins, such as AUX1 and PINs, involve distinct trafficking pathways regulated by different ARF-GEFs (62). Here, we show that basal targeting requires the GNL1-mediated early secretory process because *gnl1-1* shows resistance to ES8 at both the physiological and cellular levels. A role for GNOM that has been suggested but not yet well-studied is an additional conserved function in ER-Golgi trafficking, acting redundantly with GNL1 (33). Our finding that the GNOM-deficient mutant *van7* is also resistant to ES8 strengthens the evidence in favor of this ancestral role for GNOM. It has previously been noted that PIN1 is polarly localized in *gnl1* mutants (34); however, we demonstrate that *gnl1-1* does display a slight but significant PIN1 polarity defect. The weak nature of this defect is further consistent with a model whereby GNOM plays a redundant role with GNL1 in a trafficking route that establishes PIN1 basal polarity. An involvement of GNL1 in PIN1 endocytosis has been suggested based on the reduced BFA sensitivity of PIN1 in *gnl1* mutants (34). Based on our work, the reduced appearance of PIN1 in BFA bodies in these mutants may be more likely due to compromised polar secretion of PIN1 in the absence of either GNL1 or GNOM function, a scenario similar to that induced by ES8 treatment. However, PIN2 also showed reduced BFA sensitivity in *gnl1* mutants (34), which differs from the effects of ES8, an explanation for which could indeed be that GNL1 plays some additional role in endocytosis regulation.

Secretion has previously been shown to mediate outer lateral plasma membrane polarity in root epidermal cells (77), but evidence for a role of secretion in basal polarity has been lacking until now. Our work reveals that the early secretory pathway plays an essential role in PIN1 basal polarity establishment and thereby, to our knowledge, for the first time links secretion with basal plasma membrane polarity. Although endocytic recycling at the plasma membrane is also absolutely essential for polarity (63), ES8 does not affect this process, which depends on tight regulation by GNOM (27), suggesting that ARF-GEFs are not themselves the direct targets of ES8. It could be that ES8 affects an essential molecular component specifically involved in the ER-Golgi PIN1 trafficking pathway or, alternatively, affects some posttranslational modification to, or interacting partner of, GNL1 and GNOM. It will be interesting future work to reveal the true targets of the ES8 compounds. Because selective inhibitors of GNOM function in the early secretory route but not in the recycling pathway, the ES8 compounds showcase the power of a chemical genetics approach in dissecting complex trafficking

networks and reveal GNOM as a master regulator of basal targeting at multiple trafficking routes. In conclusion, our chemical genetics approach has revealed a role for the GNL1/GNOM-mediated early secretory pathway in PIN1 basal-directed trafficking, and the pronounced effects of the ES8 compounds on seedling growth highlight this role as being essential for regulating auxin transport and plant development.

## Materials and Methods

**Plant Material and Growth Conditions.** *A. thaliana* seedlings were grown for 5 d at 22 °C with 16 h of light per day on vertical plates of growth medium containing 1/2 MS at pH 5.6 with 0.7% agar (Duchefa Biochemie). The growth medium did not contain sucrose, unless indicated otherwise, in which case the medium was supplemented with 1% sucrose. Columbia (Col0) ecotype was used for immunolocalization, transmission electron microscopy, FM4-64 uptake, transcriptional analysis, and as WT control in seedling growth experiments, except for growth of *van7* and *osm1* seedlings, for which Landsberg *erecta* (L*er*) and C24 ecotypes were used, respectively. The *Arabidopsis* lines 35S::GFP-HDEL (78, 79), 35S::*N*-ST-YFP (79), 35S::GFP-talin (80), 35S::MAP4-GFP (81), PIN2::PIN2-GFP (82), AUX1::AUX1-YFP (83), 35S::PID21 (84), DR5rev::GFP (11), *gnl1-1* (33, 85), *van7* (48), *ben1-1* (37), *snx1-1* (39), *vps29-3* (40), *osm1* (47), CLC2::CLC2-GFP (86), SYP61::SYP61-CFP (52), RABA2a::YFP-RABA2a (87), VHA-a1::VHA-a1-GFP (88), PIN2::PIN1-GFP2 (21), XVE::PIN1 (68), and PIN1::PIN1-GFP (6) have been described previously. Due to heterozygosity, *van7* seedlings were examined under a stereomicroscope, and only those displaying a fused cotyledon phenotype were included in root-length measurements and immunolocalization experiments.

**Chemical Treatments.** Stock solutions of 50 mM BFA (Sigma-Aldrich), 10 mM ES8.0 (ID 6444878; Chembridge), 5 mM ES8.1 (ID 6540684; Chembridge), 10 mM ES8.2, ES8.3, ES8.4, ES8.5, and ES8.6 (IDs 5128188, 5267027, 7111923, 6083035, and 5128504, respectively; Chembridge), 2 mM FM4-64 (Invitrogen), 10 mM latrunculin B and estradiol (Sigma-Aldrich), and 50 mM cycloheximide (Sigma-Aldrich) were made in dimethyl sulfoxide (DMSO) and diluted in liquid 1/2 MS medium (or growth medium where indicated) for treatments of the indicated concentrations. Equal volumes of solvent were used as mock treatments for controls. For live imaging, seedlings were mounted in their treatment medium for microscopic observations. For BFA treatments, seedlings were pretreated for 30 min with ES8 before adding 25 μM BFA to the treatment for a further 90 min. For short-term ES8 treatments without BFA, seedlings were treated for 120 min. For FM4-64 and BFA cotreatments, seedlings were transferred directly after ES8 treatment to 2 μM FM4-64 in treatment medium on ice for 5 min, followed by transfer to 25 μM BFA in treatment medium at room temperature for 90 min before observation. For depolymerization of actin filaments, seedlings were pretreated for 10 min with ES8 before adding 1 μM latrunculin B to the treatment for a further 20 min. For germination and growth of seedlings on ES8 chemicals, seeds were sown directly onto ES8-supplemented growth medium. For FM4-64 uptake experiments, seedlings were transferred directly after treatment to 2 μM FM4-64 in treatment medium on ice for 5 min, followed by two washes in treatment medium on ice, and endocytosis was started by removing seedlings from ice-cold conditions. For BFA washouts, seedlings were treated with 50 μM BFA for 1 h followed by three consecutive 20-min treatment washes. For visualization of vacuolar GFP labeling, seedlings were transferred to ES8-supplemented growth medium and incubated vertically in darkness for 3 h. For induction of XVE::PIN1 expression, seedlings were transferred to growth medium supplemented with ES8 and 1 μM estradiol for 24 h, before transfer to estradiol-free liquid treatment medium for a further 5 h. For cycloheximide treatments, seedlings were pretreated for 1 h with 50 μM cycloheximide before adding ES8 to the treatment medium for a further 2 h.

**Immunolocalization and Confocal Microscopy.** Immunolocalization in *Arabidopsis* roots was performed as described previously (89) except for the fixative used, which was 4% formaldehyde, diluted from 16% formaldehyde solution (Thermo Scientific) using PBS. Blocking solution used was 3% BSA (Sigma-Aldrich). Directly after fixation, whole seedlings were transferred to the 60-well rack of an InsituPro Vsi (Intavis), where immunolocalization was performed. Seedlings were then mounted in AF1 antifadent (Citifluor). Primary antibodies used were anti-PIN1 at 1:2,000 (15) and anti-PIN2 at 1:1,000 (90). Secondary antibodies used were FITC- and CY3-conjugated anti-rabbit at 1:250 (Jackson Immunoresearch). Confocal laser-scanning microscopy was performed using Zeiss LSM 780 and Leica SP2 confocal microscopes, and all observations were made on root tips. For fluorescence recovery after photobleaching (FRAP) experiments, the mounting medium was supplemented with 1% sucrose to maintain fluorescence over several hours in the nonbleached cells, the seedlings were illuminated to prevent vacuolar GFP labeling and identical confocal acquisition and bleaching parameters between mock and chemical-treated seedlings were used. Bleaching was performed to the extent that most of the fluorescence was lost, but the individual cells and plasma membranes were still barely visible.

**Cryofixation and Transmission Electron Microscopy.** The root tips were cut from seedlings, submerged in 200 mM sucrose, 10 mM trehalose, and 10 mM Tris buffer, pH 6.6, transferred into $3.0 \times 0.5$-mm AI type A and B planchettes (Leica Microsystems), and frozen in a Leica HPM100 high pressure freezer. Freeze substitution was performed in a Leica EM AFS2 freeze substitution unit in dry acetone supplemented with 0.4% uranyl acetate at −85 °C for 16 h, followed by 5-h warm-up to −50 °C. After washing with 100% ethanol for 1 h, the roots were infiltrated and embedded in Lowicryl HM20 resin at −50 °C (intermediate steps of 30%, 50%, and 70% HM20 in ethanol, 1 h each) and polymerized for 3 d with UV light in the freeze substitution apparatus. Ultrathin sections were cut on a Leica UC 7-μL tramicrotome, post-stained with aqueous uranyl acetate/lead citrate, and examined on a Joel JEM 1230 transmission electron microscope operating at 80 kV. Micrographs were recorded with a Gatan MSC 600CW digital camera.

**Colocalization of TGN Markers.** Transgenic lines used for colocalization were obtained from SYP61::SYP61-CFP, RABA2a::YFP-RABA2a and VHA-a1::VHA-a1-GFP. F2 homozygous marker lines were screened for homozygous segregation of both markers in F3 populations. Images were acquired using a Zeiss LSM 780 confocal microscope. Image preprocessing and colocalization analysis were performed as described previously (91).

**Transcriptional Analysis.** Total RNA was extracted from 15 whole seedlings per treatment with the RNeasy kit (Qiagen). Poly(dT) cDNA was prepared from 2 μg of total RNA with SuperScript III (Invitrogen). Quantitative real-time PCR was performed with LightCycler 480 SYBR Green I Master reagents and a LightCycler 480 Real-Time PCR System (Roche Diagnostics). The following protocol was applied for the amplification of each mRNA: 5 min at 95 °C, followed by 40 cycles of 10 s at 95 °C, 15 s at 60 °C, and 20 s at 72 °C. Appropriate reference genes were selected using GeNorm (92). For reference genes and primer sequences, see Table 1. Expression levels were normalized to the reference genes TIP41-LIKE (AT4G34270) and PP2AA3 (AT1G13320), based on DCq calculations (92). For each gene of interest, the DCq values for chemical treatments were scaled to the average expression for control treatment (93–95).

**Quantitative and Statistical Analyses.** For quantification of BFA body numbers in root cells, bodies were counted for at least 100 epidermal cells, or 200 stele or cortex cells, including at least 15 seedlings, per treatment per replicate. ImageJ software (rsbweb.nih.gov/ij/) was used to measure BFA body size. For quantification of plasma membrane fluorescence intensity, confocal images were acquired using identical acquisition parameters between mock and chemical treatments. Mean gray area values along the plasma membrane

## Table 1. Primer sequences used for quantitative real-time PCR

| Gene | Forward sequence | Reverse sequence | Efficiency | Refs. |
|------|------------------|------------------|------------|-------|
| *PIN1* | TACTCCGAGACCTTCCAACTACG | TCCACCGCCACCACTTCC | 1.99 | (91) |
| *PIN2* | CCTCGCCGCACTCTTTCTTTGG | CCGTACATCGCCCTAAGCAATGG | 1.99 | (91) |
| *AUX1* | CAGGAATAGTACTTCAGATC | GAACCAAGTAATCCATCAAG | 1.77 | (92) |
| *PIP2A* | TGTGTTTTCCACTTGCTCTTTTG | CACAACGCATAAGAACCTCTTTGA | 2 | (93) |
| *TIP41-LIKE* | GGT TCC TCC TCT TGC GAT T | ACA GTT GGT GCC TCA TCT TC | 2 | — |
| *PP2AA3* | TAA CGT GGC CAA AAT GAT GC | GTT CTC CAC AAC CGC TTG GT | 2 | — |

were measured using ImageJ for at least 50 epidermal cells or 100 stele cells, including at least 15 seedlings, per treatment per replicate. For seedling root length quantification, at least 30 seedlings were measured per treatment per replicate. For quantification of FM4-64 internalization, the quotient of internal cell fluorescence compared with plasma membrane fluorescence, measured using ImageJ, was calculated per cell for at least 60 epidermal cells, including at least 10 seedlings, per treatment per replicate. For CLC2-GFP plasma membrane labeling and GFP vacuolar labeling, the percentage of epidermal cells per root with visible labeling was calculated for at least 10 roots per replicate. For quantification of TGN marker colocalization, Pearson's coefficients were calculated for at least 30 roots. For quantification of FRAP, the whole-cell fluorescence in a region of several cells, as well as the separate plasma membrane and intracellular fluorescence of a particular cell, were measured using ImageJ at precisely the same positions and focal planes for each time point directly before bleaching and once per hour from 0 to 5 h postbleach, in the bleached regions of two seedling root tips per treatment per replicate. For each root, whole-cell fluorescence was also measured at the same time points in the nonbleached region. Fluorescence values in the bleached cells were corrected according to the loss of fluorescence over time in the nonbleached cells of the same root tip and were then expressed as percentages of the prebleach value in the bleached cells. The time 0 postbleach value was then adjusted to 0, and the remaining postbleach values were corrected accordingly. For all experiments, at least three replicates were performed and always on different days. Wilcoxon rank sum (Mann–Whitney $U$) tests or Student's $t$ tests were performed on nonparametric or parametric data, respectively, to determine statistically significant differences, except for TGN marker colocalization, for which ANOVA and Tukey's honest significant difference (HSD) tests were performed.

1. Vanneste S, Friml J (2009) Auxin: A trigger for change in plant development. *Cell* 136(6):1005–1016.
2. Cheng Y, Dai X, Zhao Y (2007) Auxin synthesized by the YUCCA flavin monooxygenases is essential for embryogenesis and leaf formation in *Arabidopsis*. *Plant Cell* 19(8):2430–2439.
3. Stepanova AN, et al. (2008) TAA1-mediated auxin biosynthesis is essential for hormone crosstalk and plant development. *Cell* 133(1):177–191.
4. Tao Y, et al. (2008) Rapid synthesis of auxin via a new tryptophan-dependent pathway is required for shade avoidance in plants. *Cell* 133(1):164–176.
5. Rosquete MR, Barbez E, Kleine-Vehn J (2012) Cellular auxin homeostasis: Gatekeeping is housekeeping. *Mol Plant* 5(4):772–786.
6. Benková E, et al. (2003) Local, efflux-dependent auxin gradients as a common module for plant organ formation. *Cell* 115(5):591–602.
7. Blilou I, et al. (2005) The PIN auxin efflux facilitator network controls growth and patterning in *Arabidopsis* roots. *Nature* 433(7021):39–44.
8. Robert HS, et al. (2013) Local auxin sources orient the apical-basal axis in *Arabidopsis* embryos. *Curr Biol* 23(24):2506–2512.
9. Peer WA, Blakeslee JJ, Yang H, Murphy AS (2011) Seven things we think we know about auxin transport. *Mol Plant* 4(3):487–504.
10. Reinhardt D, et al. (2003) Regulation of phyllotaxis by polar auxin transport. *Nature* 426(6964):255–260.
11. Friml J, et al. (2003) Efflux-dependent auxin gradients establish the apical-basal axis of *Arabidopsis*. *Nature* 426(6963):147–153.
12. Friml J, et al. (2002) AtPIN4 mediates sink-driven auxin gradients and root patterning in *Arabidopsis*. *Cell* 108(5):661–673.
13. Friml J, Wiśniewska J, Benková E, Mendgen K, Palme K (2002) Lateral relocation of auxin efflux regulator PIN3 mediates tropism in *Arabidopsis*. *Nature* 415(6873): 806–809.
14. Luschnig C, Gaxiola RA, Grisafi P, Fink GR (1998) EIR1, a root-specific protein involved in auxin transport, is required for gravitropism in *Arabidopsis thaliana*. *Genes Dev* 12(14):2175–2187.
15. Gälweiler L, et al. (1998) Regulation of polar auxin transport by AtPIN1 in *Arabidopsis* vascular tissue. *Science* 282(5397):2226–2230.
16. Müller A, et al. (1998) AtPIN2 defines a locus of *Arabidopsis* for root gravitropism control. *EMBO J* 17(23):6903–6911.
17. Geisler M, et al. (2005) Cellular efflux of auxin catalyzed by the Arabidopsis MDR/PGP transporter AtPGP1. *Plant J* 44(2):179–194.
18. Blakeslee JJ, et al. (2007) Interactions among PIN-FORMED and P-glycoprotein auxin transporters in *Arabidopsis*. *Plant Cell* 19(1):131–147.
19. Terasaka K, et al. (2005) PGP4, an ATP binding cassette P-glycoprotein, catalyzes auxin transport in *Arabidopsis thaliana* roots. *Plant Cell* 17(11):2922–2939.
20. Swarup R, et al. (2001) Localization of the auxin permease AUX1 suggests two functionally distinct hormone transport pathways operate in the *Arabidopsis* root apex. *Genes Dev* 15(20):2648–2653.
21. Wiśniewska J, et al. (2006) Polar PIN localization directs auxin flow in plants. *Science* 312(5775):883.
22. Kleine-Vehn J, Friml J (2008) Polar targeting and endocytic recycling in auxin-dependent plant development. *Annu Rev Cell Dev Biol* 24(1):447–473.
23. Friml J, Benková E, Mayer U, Palme K, Muster G (2003) Automated whole mount localisation techniques for plant seedlings. *Plant J* 34(1):115–124.
24. Luschnig C, Vert G (2014) The dynamics of plant plasma membrane proteins: PINs and beyond. *Development* 141(15):2924–2938.
25. Dhonukshe P, et al. (2007) Clathrin-mediated constitutive endocytosis of PIN auxin efflux carriers in *Arabidopsis*. *Curr Biol* 17(6):520–527.
26. Kitakura S, et al. (2011) Clathrin mediates endocytosis and polar distribution of PIN auxin transporters in *Arabidopsis*. *Plant Cell* 23(5):1920–1931.
27. Geldner N, et al. (2003) The *Arabidopsis* GNOM ARF-GEF mediates endosomal recycling, auxin transport, and auxin-dependent plant growth. *Cell* 112(2):219–230.
28. Naramoto S, et al. (2010) ADP-ribosylation factor machinery mediates endocytosis in plant cells. *Proc Natl Acad Sci USA* 107(50):21890–21895.
29. Steinmann T, et al. (1999) Coordinated polar localization of auxin efflux carrier PIN1 by GNOM ARF GEF. *Science* 286(5438):316–318.
30. Kleine-Vehn J, Dhonukshe P, Swarup R, Bennett M, Friml J (2006) Subcellular trafficking of the *Arabidopsis* auxin influx carrier AUX1 uses a novel pathway distinct from PIN1. *Plant Cell* 18(11):3171–3181.
31. Fischer U, et al. (2006) Vectorial information for *Arabidopsis* planar polarity is mediated by combined *AUX1*, *EIN2*, and *GNOM* activity. *Curr Biol* 16(21):2143–2149.
32. Grebe M, et al. (2002) Cell polarity signaling in *Arabidopsis* involves a BFA-sensitive auxin influx pathway. *Curr Biol* 12(4):329–334.
33. Richter S, et al. (2007) Functional diversification of closely related ARF-GEFs in protein secretion and recycling. *Nature* 448(7152):488–492.
34. Teh OK, Moore I (2007) An ARF-GEF acting at the Golgi and in selective endocytosis in polarized plant cells. *Nature* 448(7152):493–496.
35. Naramoto S, et al. (2014) Insights into the localization and function of the membrane trafficking regulator GNOM ARF-GEF at the Golgi apparatus in Arabidopsis. *Plant Cell* 26(7):3062–3076.
36. Richter S, et al. (2012) Polarized cell growth in *Arabidopsis* requires endosomal recycling mediated by GBF1-related ARF exchange factors. *Nat Cell Biol* 14(1):80–86.
37. Tanaka H, Kitakura S, De Rycke R, De Groodt R, Friml J (2009) Fluorescence imaging-based screen identifies ARF GEF component of early endosomal trafficking. *Curr Biol* 19(5):391–397.
38. Richter S, et al. (2014) Delivery of endocytosed proteins to the cell-division plane requires change of pathway from recycling to secretion. *eLife* 3:e02131.
39. Jaillais Y, Fobis-Loisy I, Miège C, Rollin C, Gaude T (2006) AtSNX1 defines an endosome for auxin-carrier trafficking in *Arabidopsis*. *Nature* 443(7107):106–109.
40. Jaillais Y, et al. (2007) The retromer protein VPS29 links cell polarity and organ initiation in plants. *Cell* 130(6):1057–1070.
41. Jaillais Y, Fobis-Loisy I, Miège C, Gaude T (2008) Evidence for a sorting endosome in *Arabidopsis* root cells. *Plant J* 53(2):237–247.
42. Kleine-Vehn J, et al. (2008) Differential degradation of PIN2 auxin efflux carrier by retromer-dependent vacuolar targeting. *Proc Natl Acad Sci USA* 105(46): 17812–17817.
43. Nodzyński T, et al. (2013) Retromer subunits VPS35A and VPS29 mediate prevacuolar compartment (PVC) function in *Arabidopsis*. *Mol Plant* 6(6):1849–1862.
44. Friml J, et al. (2004) A PINOID-dependent binary switch in apical-basal PIN polar targeting directs auxin efflux. *Science* 306(5697):862–865.
45. Michniewicz M, et al. (2007) Antagonistic regulation of PIN phosphorylation by PP2A and PINOID directs auxin flux. *Cell* 130(6):1044–1056.
46. Kleine-Vehn J, et al. (2009) PIN auxin efflux carrier polarity is regulated by PINOID kinase-mediated recruitment into GNOM-independent trafficking in *Arabidopsis*. *Plant Cell* 21(12):3839–3849.
47. Zhu J, et al. (2002) OSM1/SYP61: A syntaxin protein in Arabidopsis controls abscisic acid-mediated and non-abscisic acid-mediated responses to abiotic stress. *Plant Cell* 14(12):3009–3028.
48. Koizumi K, Sugiyama M, Fukuda H (2000) A series of novel mutants of *Arabidopsis thaliana* that are defective in the formation of continuous vascular network: Calling the auxin signal flow canalization hypothesis into question. *Development* 127(15): 3197–3204.
49. Yamauchi Y, Fukaki H, Fujisawa H, Tasaka M (1997) Mutations in the *SGR4*, *SGR5* and *SGR6* loci of *Arabidopsis thaliana* alter the shoot gravitropism. *Plant Cell Physiol* 38(5): 530–535.
50. Mayer U, Torres Ruiz RA, Berleth T, Miséra S, Jürgens G (1991) Mutations affecting body organization in the *Arabidopsis* embryo. *Nature* 353:402–407.
51. Tanaka H, et al. (2014) BEX1/ARF1A1C is required for BFA-sensitive recycling of PIN auxin transporters and auxin-mediated development in Arabidopsis. *Plant Cell Physiol* 55(4):737–749.

52. Robert S, et al. (2008) Endosidin1 defines a compartment involved in endocytosis of the brassinosteroid receptor BRI1 and the auxin transporters PIN2 and AUX1. *Proc Natl Acad Sci USA* 105(24):8464–8469.

53. Drakakaki G, et al. (2011) Clusters of bioactive compounds target dynamic endomembrane networks in vivo. *Proc Natl Acad Sci USA* 108(43):17850–17855.

54. Surpin M, et al. (2005) The power of chemical genomics to study the link between endomembrane system components and the gravitropic response. *Proc Natl Acad Sci USA* 102(13):4902–4907.

55. Rojas-Pierce M, et al. (2007) *Arabidopsis* P-glycoprotein19 participates in the inhibition of gravitropism by gravacin. *Chem Biol* 14(12):1366–1376.

56. Norambuena L, Zouhar J, Hicks GR, Raikhel NV (2008) Identification of cellular pathways affected by Sortin2, a synthetic compound that affects protein targeting to the vacuole in *Saccharomyces cerevisiae*. *BMC Chem Biol* 8:1.

57. Zouhar J, Hicks GR, Raikhel NV (2004) Sorting inhibitors (Sortins): Chemical compounds to study vacuolar sorting in *Arabidopsis*. *Proc Natl Acad Sci USA* 101(25): 9497–9501.

58. Sorieul M, et al. (2011) An Exo2 derivative affects ER and Golgi morphology and vacuolar sorting in a tissue-specific manner in *arabidopsis*. *Traffic* 12(11):1552–1562.

59. Geldner N, Friml J, Stierhof Y-D, Jürgens G, Palme K (2001) Auxin transport inhibitors block PIN1 cycling and vesicle trafficking. *Nature* 413(6854):425–428.

60. Silady RA, et al. (2008) The GRV2/RME-8 protein of Arabidopsis functions in the late endocytic pathway and is required for vacuolar membrane flow. *Plant J* 53(1):29–41.

61. Feraru E, et al. (2010) The AP-3 β adaptin mediates the biogenesis and function of lytic vacuoles in *Arabidopsis*. *Plant Cell* 22(8):2812–2824.

62. Kleine-Vehn J, et al. (2008) ARF GEF-dependent transcytosis and polar delivery of PIN auxin carriers in *Arabidopsis*. *Curr Biol* 18(7):526–531.

63. Kleine-Vehn J, et al. (2011) Recycling, clustering, and endocytosis jointly maintain PIN auxin carrier polarity at the plasma membrane. *Mol Syst Biol* 7(1):540.

64. Ueda T, Yamaguchi M, Uchimiya H, Nakano A (2001) Ara6, a plant-unique novel type Rab GTPase, functions in the endocytic pathway of *Arabidopsis thaliana*. *EMBO J* 20(17):4730–4741.

65. Kang B-H, Nielsen E, Preuss ML, Mastronarde D, Staehelin LA (2011) Electron tomography of RabA4b- and PI-4Kβ1-labeled *trans* Golgi network compartments in *Arabidopsis*. *Traffic* 12(3):313–329.

66. Tamura K, et al. (2003) Why green fluorescent fusion proteins have not been observed in the vacuoles of higher plants. *Plant J* 35(4):545–555.

67. Laxmi A, Pan J, Morsy M, Chen R (2008) Light plays an essential role in intracellular distribution of auxin efflux carrier PIN2 in *Arabidopsis thaliana*. *PLoS One* 3(1):e1510.

68. Petrásek J, et al. (2006) PIN proteins perform a rate-limiting function in cellular auxin efflux. *Science* 312(5775):914–918.

69. Hicks GR, Raikhel NV (2010) Advances in dissecting endomembrane trafficking with small molecules. *Curr Opin Plant Biol* 13(6):706–713.

70. Dhonukshe P, Jiang L, Schumacher K (2008) Auxin transport inhibitors impair vesicle motility and actin cytoskeleton dynamics in diverse eukaryotes. *Proc Natl Acad Sci USA* 105(11): 4489–4494.

71. Robinson DG, Jiang L, Schumacher K (2008) The endosomal system of plants: Charting new and familiar territories. *Plant Physiol* 147(4):1482–1492.

72. Hicks GR, Raikhel NV (2009) Opportunities and challenges in plant chemical biology. *Nat Chem Biol* 5(5):268–272.

73. Bailly A, et al. (2008) Modulation of P-glycoproteins by auxin transport inhibitors is mediated by interaction with immunophilins. *J Biol Chem* 283(31):21817–21826.

74. Kim J-Y, et al. (2010) Identification of an ABCB/P-glycoprotein-specific inhibitor of auxin transport by chemical genomics. *J Biol Chem* 285(30):23309–23317.

75. Anders N, Jürgens G (2008) Large ARF guanine nucleotide exchange factors in membrane trafficking. *Cell Mol Life Sci* 65(21):3433–3445.

76. Shin H-W, Nakayama K (2004) Guanine nucleotide-exchange factors for arf GTPases: Their diverse functions in membrane traffic. *J Biochem* 136(6):761–767.

77. Łangowski L, Růzicka K, Naramoto S, Kleine-Vehn J, Friml J (2010) Trafficking to the outer polar domain defines the root-soil interface. *Curr Biol* 20(10):904–908.

78. Haseloff J, Siemering KR, Prasher DC, Hodge S (1997) Removal of a cryptic intron and subcellular localization of green fluorescent protein are required to mark transgenic *Arabidopsis* plants brightly. *Proc Natl Acad Sci USA* 94(6):2122–2127.

79. Grebe M, et al. (2003) *Arabidopsis* sterol endocytosis involves actin-mediated trafficking via ARA6-positive early endosomes. *Curr Biol* 13(16):1378–1387.

80. Kost B, Spielhofer P, Chua NH (1998) A GFP-mouse talin fusion protein labels plant actin filaments *in vivo* and visualizes the actin cytoskeleton in growing pollen tubes. *Plant J* 16(3):393–401.

81. Marc J, et al. (1998) A GFP-MAP4 reporter gene for visualizing cortical microtubule rearrangements in living epidermal cells. *Plant Cell* 10(11):1927–1940.

82. Xu J, Scheres B (2005) Dissection of Arabidopsis ADP-RIBOSYLATION FACTOR 1 function in epidermal cell polarity. *Plant Cell* 17(2):525–536.

83. Swarup R, et al. (2004) Structure-function analysis of the presumptive Arabidopsis auxin permease AUX1. *Plant Cell* 16(11):3069–3083.

84. Benjamins R, Quint A, Weijers D, Hooykaas P, Offringa R (2001) The PINOID protein kinase regulates organ development in *Arabidopsis* by enhancing polar auxin transport. *Development* 128(20):4057–4067.

85. Ríos G, et al. (2002) Rapid identification of *Arabidopsis* insertion mutants by non-radioactive detection of T-DNA tagged genes. *Plant J* 32(2):243–253.

86. Konopka CA, Bednarek SY (2008) Variable-angle epifluorescence microscopy: A new way to look at protein dynamics in the plant cell cortex. *Plant J* 53(1):186–196.

87. Chow CM, Neto H, Foucart C, Moore I (2008) Rab-A2 and Rab-A3 GTPases define a *trans*-golgi endosomal membrane domain in *Arabidopsis* that contributes substantially to the cell plate. *Plant Cell* 20(1):101–123.

88. Dettmer J, Hong-Hermesdorf A, Stierhof YD, Schumacher K (2006) Vacuolar H$^+$-ATPase activity is required for endocytic and secretory trafficking in *Arabidopsis*. *Plant Cell* 18(3): 715–730.

89. Sauer M, Paciorek T, Benková E, Friml J (2006) Immunocytochemical techniques for whole-mount *in situ* protein localization in plants. *Nat Protoc* 1(1):98–103.

90. Abas L, et al. (2006) Intracellular trafficking and proteolysis of the *Arabidopsis* auxin-efflux facilitator PIN2 are involved in root gravitropism. *Nat Cell Biol* 8(3):249–256.

91. Vain T, et al. (2014) The cellulase KORRIGAN is part of the Cellulose Synthase Complex. *Plant Physiol* 165(4):1521–1532.

92. Vandesompele J et al. (2002) Accurate normalization of real-time quantitative RT-PCR data by geometric averaging of multiple internal control genes. *Genome Biol* 3(7): RESEARCH0034.

93. Růžička K, et al. (2009) Cytokinin regulates root meristem activity via modulation of the polar auxin transport. *Proc Natl Acad Sci USA* 106(11):4284–4289.

94. Yu J, Wen CK (2013) Arabidopsis *aux1$^{rcr1}$* mutation alters AUXIN RESISTANT1 targeting and prevents expression of the auxin reporter *DR5:GUS* in the root apex. *J Exp Bot* 64(4):921–933.

95. Péret B, et al. (2012) Auxin regulates aquaporin function to facilitate lateral root emergence. *Nat Cell Biol* 14(10):991–998.